10th International Symposium on Practical Design of Ships and Other Floating Structures
Houston, Texas, United States of America

Hydrodynamic Pressure and Structural Loading of High-Speed Catamaran and SES

William S. Vorus[1)], Robert D. Sedat[2)]

[1)] School of NAME, University of New Orleans, New Orleans, LA
[2)] US Coast Guard R&D Center, Groton, CT

Abstract

A theory and engineering model for seaway dynamic response of high-speed catamaran and SES hull forms was developed and applied to configurations of interest. Zero gravity semi-planing theory was used initially for both calm-water analysis and seaway dynamics. From this initial work it was concluded that while the typical operating Froude number of the larger vessels of interest is high (slightly above unity), it is probably not high enough to justify discarding the effects of gravity in the hydrodynamics. A main effort was then to incorporate gravity into the hydrodynamics, for both calm water operations and in waves. The Mauro "flat ship" theory was found to be useful as the basis for this extension. The development is demonstrated by comparing calculations from the extended code to the model experiments conducted on the Bell-Halter110 SES at the old Lockheed tank in San Diego, CA back in the 1970's.

Keywords

Catamaran; Hydrodynamics; Resistance; Seakeeping; SES.

Introduction

The criteria most widely available to the design community for determining hydrodynamic forces and hull surface pressure for use in vessel design are embodied in Guidelines and Rules promulgated by the various Classification Societies. When applied to fast multi-hull designs, with service speeds of 50 to 60 knots or higher, formulas published by ABS, DnV, and Lloyd's Register (for example) may produce significantly different values of design and impact pressure loads. This produces a corresponding variation in scantling requirements, particularly for hulls with sandwich-skin composite construction.

It was recognized as a worthwhile service to the ship design community to develop a comprehensive tool for evaluation of high-speed catamaran and catamaran/SES design pressure and wave impact loading. Ideally, this tool should be based on an analytical/numerical model, developed from first principles, and validated by comparison with test data for the hull types of interest. Such an analysis tool has been developed and has been applied to the Bell-Halter 110 ft SES built in the late 1970's. Both calm water and seaway model test data was available here for making definitive comparisons with the calculations.

Approach

The base computer codes employed, that implement the general hydrodynamics outlined above, existed originally in the VAI EDITH system. EDITH (Engineering Development in Theoretical Hydrodynamics) is a computer system dedicated to the application of sound theoretical hydrodynamics to relevant engineering challenges in marine hydrodynamics. With regard to the work described here, the relevant EDITH code was the pre-existing EDITH 2, or CatSea, for analysis of high speed planning catamarans.

The new code series assembled for the SES analysis is EDITH 2-AG, or CatSeaAir.

All of the EDITH-series algorithms prior to EDITH 2-AG had implemented the zero gravity high-speed theory of Vorus(1996). The new CatSeaAir code was adapted for approximate inclusion of vessel generated gravity waves, and now that algorithm has been back-fit into the other programs of the series.

Non-zero Gravity Theory

The base theory used here for gravity wave effects is the linearized planning monohull theory of Maruo (1967), adapted for bi-hulls, including SES. The Maruo formulation is based on ideal flow theory and represents a solution to the Laplace equation for a velocity potential subject to the linearized free-surface boundary condition, with gravity included, and a radiation condition of no waves upstream. It is a steady flow theory, and therein lies the major approximation of this application. The unsteady seaway dynamics of EDITH 2-AG assumes that the wave-making is quasi-steady.

That is, with changing vessel attitudes in the seaway, this application assumes that at any instant the temporal effects in the wave-making, as regards loading changes, are small. The unsteady effects in the wave making are generated by the Maruo solution at any instant for the craft geometry varying generally with time.

Referring to Figure 1, x is downstream with the coordinate system located at the bow, and y is up. The planing surface is considered to occupy the region of the y = 0 plane corresponding to $-Z(x) \le z \le -Z_k$ and $Z_k \le z \le Z(x)$ with $0 \le x \le L$,L being the instantaneous waterline length. Z(x) is the waterline offset and Zk is the demi-hull keel offset, taken as constant in x. The kinematic boundary condition is satisfied on this plane surface, which requires that the craft bottom have a flat characterization. Planing craft are consistent with the assumption of flatness in satisfying boundary conditions on the y = 0 plane, and this has been a universal assumption for conventional analysis of planing craft at zero gravity, as built upon the original work of vonKarman(1929) and Wagner (1932). The current CatSeaAir code uses the non-linear slender-body formulation of Vorus (1996), with the addition of the specially adapted Mauro gravity routines.

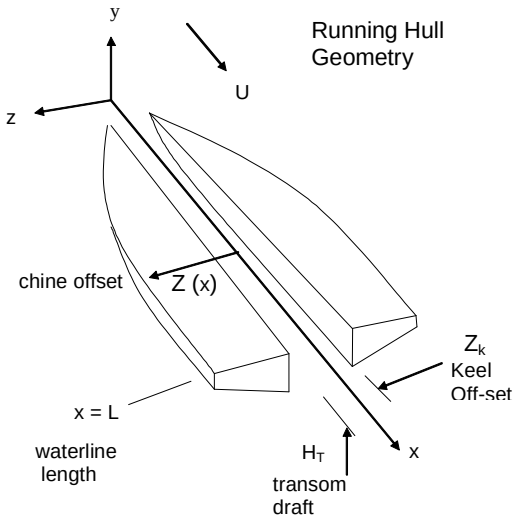

Fig 1: Catamaran/SES Geometry

The Maruo velocity potential, adapted for the catamaran geometry, is:

$$\Phi(x, y, z) = -\frac{1}{\pi} \int_{\zeta=-Z(x)}^{-Z_k} +$$

$$\int_{Z_k}^{Z(x)} \int_{\xi=0}^{x} \gamma_z(\xi, \zeta) \int_{\lambda=0}^{\infty} \cos\left[\sqrt{\kappa\lambda}(x-\xi)\right] \cos\left[\lambda(z-\zeta)\right] e^{\lambda y} d\lambda d\xi d\zeta \quad (1)$$

Referring back to Figure 1, Φ is the velocity potential in the fluid region, $y \le 0$. γ_z is the unknown transverse (z-directed) vortex density component on the surface projection. (The companion axial vortex density component, γ_x, is the usual subject of the conventional zero gravity slender body formulation of planing, but the two components are related by the condition of zero divergence of the two dimensional surface vector.)
κ in (1) is the wave number:

$$\kappa = g/U^2 \quad (2)$$

κ entered the derivation of (1) in satisfying the linearized free surface boundary condition in allowing for gravity wave generation.

Note from (1) that only the sections at $\xi <$ x upstream convect into the current x – solution section; γ_z for $\xi <$ x will always be known from upstream computation steps. This x-marching characteristic of the elliptic solutions in the z-coordinate is common to the parabolic reduction in x associated with all slender body theories.

The linearized kinematic boundary condition to be satisfied on the craft surface projection is:

$$\frac{\partial \Phi}{\partial y} = U \frac{\partial y_0}{\partial x} \qquad \text{on y =}$$

$$0, -Z(x) \le z \le -Z_k \text{ and } Z_k \le z \le Z(x), \; 0 \le x \le L \quad (3)$$

$y_0(x,z)$ is the definition of the planing surface $y - y_0(x,z) = 0$, which is presumed to be known for purposes of the theoretical development.

Substitution of (1) into (3) produces an integral equation that is solved numerically for the vortex density $\gamma_Z(x, z)$. This solution is difficult in that it exhibits a higher order singularity that must be carefully treated, Tuck (1975). But it is made easier by the downstream marching, for which each successive x-station is solved in terms of the already available solutions from the stations upstream.

The axial perturbation velocity on the surface is given in terms of $\gamma_Z(x, z)$ as:

$$u(x, z) = -\gamma_Z(x, z) \quad (4)$$

The coefficient of pressure on the surface is then:

$$C_p(x, z) = -2\left(\frac{u}{U}\right) \quad (5)$$

This pressure distribution, (5), is integrated over the surface to produce the force components needed in Newton's Law for stepping the vessel motion to the next time.

Note that $\kappa \to 0$ corresponds to vanishing gravity by (2). $\kappa = 0$ in (1) therefore gives the zero gravity solution $\gamma_{zi}(x, z)$. The vortex density due only to waves is therefore:

$$\gamma_{zw} = \gamma_z - \gamma_{zi} \quad (6)$$

(5) and (6) give the pressure due to wave-making as:

$$C_{pw}(x,z) = 2\left(\frac{\gamma_{zw}(x,z)}{U}\right) \qquad (7)$$

A subroutine has been added in CatSeaAir to solve (1) and (3) and to compute (7) at each time step as the hull wetted geometry changes. $C_{pw}(x,z)$ is added to the g = 0 surface pressure currently calculated in CatSeaAir to obtain the total pressure field including the gravity wave effects.

Hydrostatic pressure relative to the undisturbed water surface is also included in the pressure sum in CatSeaAir, as well as is air pressure associated with SES operations.

The new version of CatSeaAir with the gravity routines included (as an option under user control) is designated as EDITH 2-AG.

EDITH 2-AG is simple to execute and interpret. However, with the gravity option exercised, the code is time consuming. It executes about 200 time steps per hour. With 10,000 to 20,000 time steps desirable for achieving statistically stationary conditions in a random seaway analysis, approximately 50 to 100 hours of running time is required. This is on a 3.2 Ghz workstation. Most of the calculation is serial in x and then serial in time, so it is not clear that parallel processing (or cluster computing) would help much. With the gravity option off, CatSeaAir runs about 20 time steps per minute.

The extended code is robust, however, and never crashes and it has a restart capability. Effort will be made, by programming refinements, to reduce the time consumption requirement as time permits.

Comparison of Code Predictions with Model Tests

The EDITH 2-AG CatSeaAir code was applied to the Bell-Halter 110 ft SES. This design was extensively model tested in the 1970's at the old Lockheed, San Diego facility (LOLTB), as reported in LMSC/D682700, December 1979. Fig. 2 is the arrangement of the 1/15-scale (7 ft) model that was tested. Figs. 3a and 3b are the body plan from which the geometry input for CatSeaAir was extracted. Note from Figs. 2 and 3 that the BH110 is a "rockered" hull with 2.6 degree of keel rocker aft.

Analysis versus Experiments - Calm-Water

The model experiments in calm water reported the following data needed for comparison with the analysis:

Steady speed, U

Weight, W

Longitudinal center of gravity, xcg

Air cushion pressure, p_{ac}

Transom draft, Ht/Zk

Trim

Drag coefficient, Cd

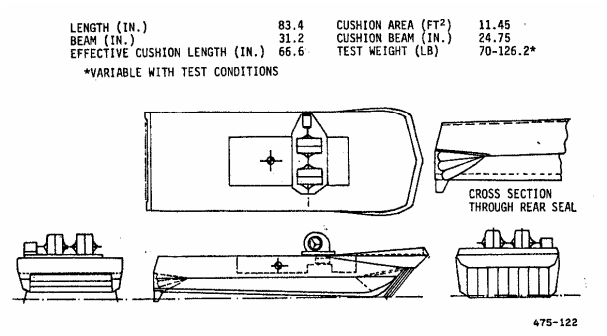

Fig 2: BH 110 Test Model

From the above list the % air support, WA, was obtained from the cushion pressure by multiplying p_{ac} by the cushion ceiling area and dividing by the model weight, W. The transom draft was extrapolated from the measured mid-cushion draft using the measured trim angle.

The theoretical model has three degrees of freedom: heave, pitch, and surge. But the physical model tested was restrained in surge, so that drag represents the surge equation. This requires that of the seven variables listed above only three can be predicted by CatSeaAir and the others must be considered as input to the analysis. The normal choice for input would be U, W, xcg, and WA, with the trim, transom draft and drag considered as output to be compared with the test measurements. This is the context of the experimental data presentation.

However, with trim, draft, and drag as the output, the calculations were very poorly behaved in some cases and failed to converge to reasonable values, if at all, in others. After a great deal of calculation it was decided that xcg and WA given for the tests were not uniformly consistent. WA had to be estimated from the cushion pressure measurement by assuming the cushion pressure uniform and constant over the wet deck. There was also some seeming confusion over the experimental xcg determination. Two xcg's were reported; one in air and a CG in "hover" on the air cushion at zero forward speed. They were different and it was not always clear which was being reported. These tests were conducted 30 years ago, and while one or two of the TEXTRON people involved were still available and helpful, the xcg issue, particularly, remained confusing.

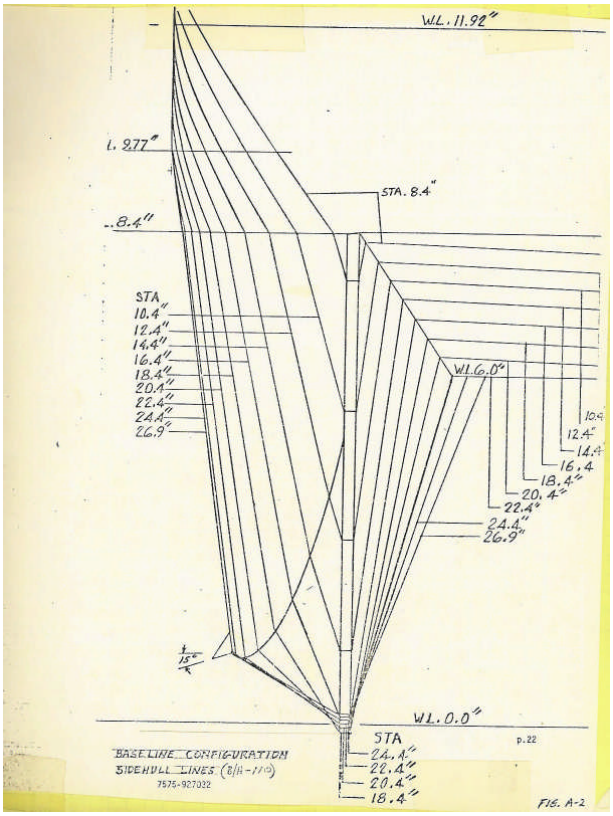

Figure 3a: BH110 (Model B-34C) Body Plan Forward

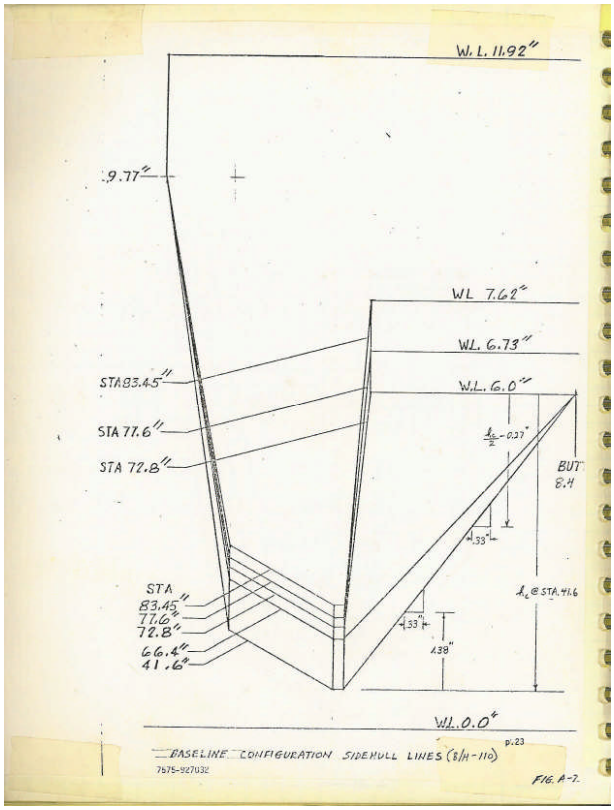

Figure 3b: BH110 (Model B-34C) Body Plan Aft

It was therefore finally decided to take the trim and draft as the two input variables, along with U and W, for the calm water analysis, and to calculate WA, xg and Cd for comparison to the test data. This result is reported below in Table 1 for the three model weights of Condition 1: W = 70, 81.5, and 93 lbs.

Table 1: BH 110 Calm Water Runs, Model B34C, Configuration 1 LMSC/D682700, 12/79, Book 5 VAI Analysis of 9-06

No.	U(fps)	Vfs(k)	W(#)	%xge	Trim	Ht	Cl	%WAe	%WAc	xcge	xcgc	%xcgc	Cde	Cdc
362	12.91	29.60	70.0	0.0	1.28	0.1229	0.3935	87.5	81.0	2.623	2.485	-2.61	0.0233	0.0169
363	17.26	39.58	70.0	0.0	0.57	0.0785	0.2202	85.5	78.8	2.623	2.713	1.70	0.0126	0.0194
364	13.10	30.04	70.0	-0.7	1.59	0.1273	0.3822	78.7	81.9	2.586	2.465	-2.99	0.0221	0.0158
365	17.48	40.08	70.0	-0.7	0.97	0.0874	0.2147	83.7	82.9	2.586	2.499	-2.52	0.0103	0.0118
366	24.28	55.68	70.0	-1.5	0.75	0.0738	0.1113	81.7	86.3	2.544	2.536	-1.65	0.0069	0.0095
367	13.12	30.08	70.0	-1.5	1.81	0.1407	0.3811	85.0	81.9	2.544	2.466	-2.97	0.0215	0.0161
368	17.48	40.08	70.0	-1.5	1.17	0.1012	0.2147	82.9	82.7	2.544	2.498	-2.37	0.0108	0.0118
370	24.08	55.22	70.0	-2.0	0.88	0.0823	0.1131	78.4	85.4	2.517	2.526	-1.84	0.0068	0.0094
371	30.90	70.86	70.0	-2.0	0.63	0.0634	0.0687	75.4	86.8	2.517	2.554	-1.31	0.0049	0.0083
372	9.20	21.10	70.0	-0.5	2.27	0.1233	0.7751	82.6	87.0	2.597	2.433	-3.60	0.0409	0.0216
378	17.32	39.72	70.0	-1.0	1.00	0.0941	0.2187	82.0	84.4	2.571	2.502	-2.29	0.0102	0.0120
393	17.40	39.90	70.0	-1.0	1.14	0.0980	0.2168	86.7	83.0	2.571	2.495	-2.42	0.0106	0.0117
397	9.15	20.98	81.5	0.0	2.48	0.2307	0.9125	86.5	75.0	2.623	2.459	-3.10	0.0549	0.0393
398	13.08	30.00	81.5	0.0	1.45	0.1315	0.4465	89.1	79.1	2.623	2.478	-2.74	0.0268	0.0183
399	9.15	20.98	81.5	-0.5	2.68	0.2374	0.9125	85.2	75.0	2.597	2.458	-3.12	0.0562	0.0397
400	13.08	30.00	81.5	-0.5	1.74	0.1344	0.4465	87.7	82.3	2.597	2.460	-3.08	0.0251	0.0173
401	17.41	39.92	81.5	-0.5	0.98	0.0984	0.2509	86.3	83.3	2.597	2.520	-1.95	0.0132	0.0134
402	24.00	55.03	81.5	-0.5	0.61	0.0777	0.1326	85.1	79.5	2.597	2.743	2.27	0.0088	0.0145
403	13.10	30.04	81.5	-1.0	1.96	0.1499	0.4451	87.4	81.9	2.571	2.462	-3.05	0.0252	0.0178
404	17.44	39.99	81.5	-1.0	1.22	0.1103	0.2509	84.7	81.5	2.571	2.504	-2.25	0.0117	0.0130
405	24.06	55.17	81.5	-1.0	0.85	0.0834	0.1320	84.0	85.4	2.571	2.537	-1.63	0.0080	0.0100
406	12.35	28.32	81.5	-1.5	2.37	0.1775	0.5008	85.4	81.3	2.544	2.458	-3.12	0.0302	0.0205
407	17.43	39.97	81.5	-1.5	1.38	0.1113	0.2514	83.6	83.4	2.544	2.488	-2.55	0.0122	0.0123
408	24.08	55.17	81.5	-1.5	0.94	0.0830	0.1317	81.1	84.4	2.544	2.523	-1.89	0.0074	0.0097
416	17.40	39.90	81.5	-1.0	1.24	0.1104	0.2524	84.3	81.8	2.571	2.501	-2.31	0.0114	0.0129
422	9.08	20.82	81.5	0.5	2.30	0.2215	0.9265	85.9	74.6	2.649	2.469	-2.91	0.0543	0.0398
423	23.89	54.78	81.5	-2.0	1.05	0.0953	0.1339	81.4	83.0	2.517	2.531	-1.74	0.0074	0.0102
425	9.16	21.00	93.0	0.0	2.75	0.2617	1.0380	85.4	73.8	2.623	2.469	-2.91	0.0657	0.0485
426	13.09	30.02	93.0	0.0	1.75	0.1500	0.5082	86.7	79.8	2.623	2.469	-2.91	0.0299	0.0203
434	13.09	30.02	93.0	-0.5	1.99	0.1517	0.5082	86.5	82.1	2.597	2.457	-3.14	0.0293	0.0195
435	17.29	39.65	93.0	-0.5	1.17	0.1125	0.2913	83.6	83.0	2.597	2.506	-2.21	0.0135	0.0142
436	17.42	39.95	93.0	-1.0	1.40	0.1160	0.2870	84.4	82.9	2.571	2.489	-2.54	0.0131	0.0133
437	17.44	39.99	93.0	-1.5	1.54	0.1271	0.2863	83.4	82.4	2.544	2.493	-2.46	0.0312	0.0135

Key:

No. run number from test book 5

U: model speed in tank

Vfs: Froude scaled full scale speed in knots

W: weight of model, lbs

%xg: xcg shift as % of cushion length from cushion center from report

Trim: trim angle, deg, from report *(input)*

Ht: transom draft/Yk; Yk demi-hull keel offset from report *(input)*

Cl: hull lift coefficient, $W/1/2\rho U^2 Yk^2$ (*calc*)

%WA: percent of W supported by air (*experimental and calc*)

xcg: location of center of gravity forward of transom/Yk (*experimental and calc*)

Cd: hull drag coefficient, $D/1/2\rho U^2 Yk^2$ (*experimental and calc*)

sub – e: experimental

sub – c: CatSeaAir calculation

Description of the data is provided above below the table. The comparisons were made for all of the data for model Condition 1. The differences in the several Conditions are generally superficial non-systematic variations in the model. Condition 1 was considered adequate coverage.

Choosing not to invert the equations of motion for steady trim and transom draft avoided the time stepping and actually made the CatSeaAir calculations much simpler. CatSeaAir was first run with WA set to zero with the trim and draft set to the Table 1 measured values. This produced W_h and xcg_h, with W_h being the weight supported by hydrodynamics/hydrostatics with zero air cushion pressure at the given trim and draft, with xcg_h being the center of application of W_h. Weight and moment component summation gives:

$$1 = \frac{WA}{W} + \frac{W_h}{W} \qquad (8)$$

$$xcg = \frac{WA}{W} xcg_A + \frac{W_h}{W} xcg_h \qquad (9)$$

with xcg_A being the known center of the air cushion from the transom.

Equation (8) is first solved for WA/W, which is substituted into (9) to calculate the required xcg. These are the values listed in Table 1 as %WAc and %xcgc[1].

Fig 4a and 4b are plots of the trim and draft input values from Table 1 for each of the three model weights.

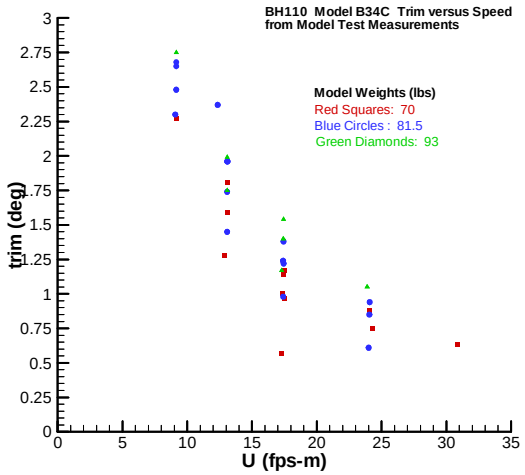

Fig 4a: Measured Trim versus Speed for the Three Model Test Weights of 70, 81.5 and 93 lbs.

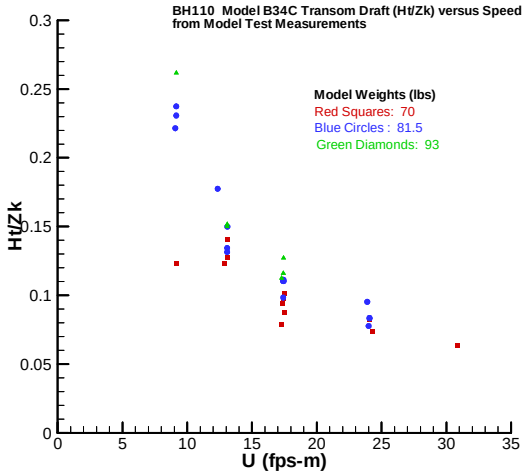

Fig 4b: Measured Transom Draft versus Speed for the Three Model Test Weights of 70, 81.5 and 93 lbs.

The Table 1 data displayed on Fig 4a and Fig 4b is difficult to plot as conventional curves versus speed because so much is varying. Some of the variation is systematic input variation and some seems to be random experimental variability. It seems to be best displayed

[1] $\%xcg = 100(xcg - xcg_A)/xcg_A$

in terms of the unconnected data points as "scatter graphs," as on Fig 4. The interpretation of Fig 4, and of the additional scatter graphs to follow, is that the degree of cluster at any speed reflects the degree of data consistency, with high cluster reflecting high consistency. Spreading vertically does correctly occur due to the xcg variations.

It must be kept in mind that the trim and draft data of Fig 4 is considered the input data from the experiments.

So the calculated output from this input, via CatSeaAir, should reflect, at best, the same level of scatter.

Figs 5 to 10 are the calculated WA fraction and %xcg forward of mid-cushion from (8) and (9) via the Table 1 runs for each of the three weights.

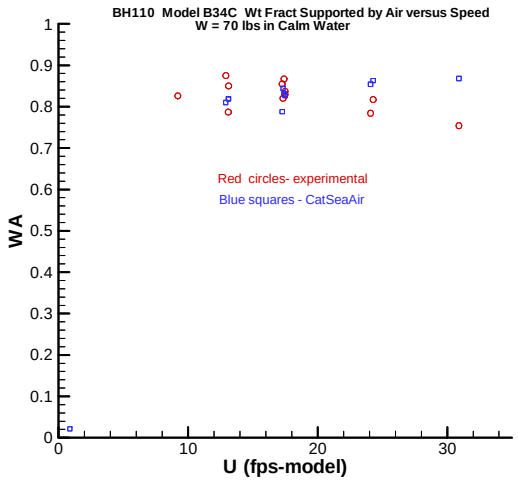

Fig 5: Calculated WA/W versus Model Speed for 70 lb Model

The calculated WA/W displayed on Figs 5, 6, and 7 are considered to be quite close to the experimental in consideration of the variability of the input trim and transom draft measurements displayed on Fig 4.

As for the xcg data on Figs 8, 9, and 10, the test values were considered to be part of the experimental set-up. Except for a few irregular points, the xcg implied by CatSeaAir are slightly lower (xcg further aft) and the variability, or sensitivity to speed differences, seems to be lower, in general. It should be kept in mind that a 1% CG shift is only about 3/8 inch relative to the length of the 7-foot model. It seems likely that movements of this magnitude would be hard to set by the simple balance and leveling methods used. And then there was uncertainty about “in air” or “in hover” cited in the preceding.

The xcg comparisons are considered to contribute to establishing the validity of CatSeaAir, and not to diminish it.

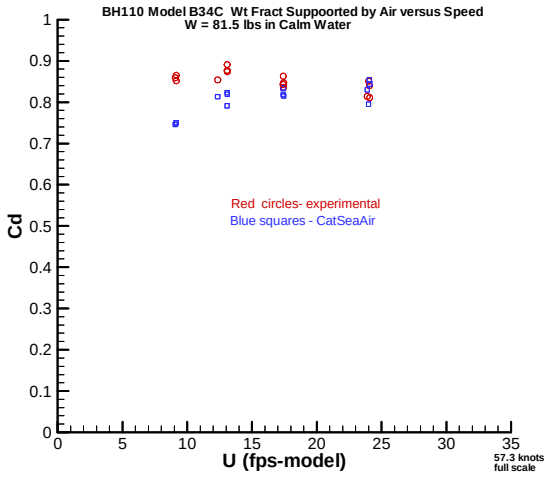

Fig 6: Calculated WA/W versus Model Speed for 81.5 lb Model

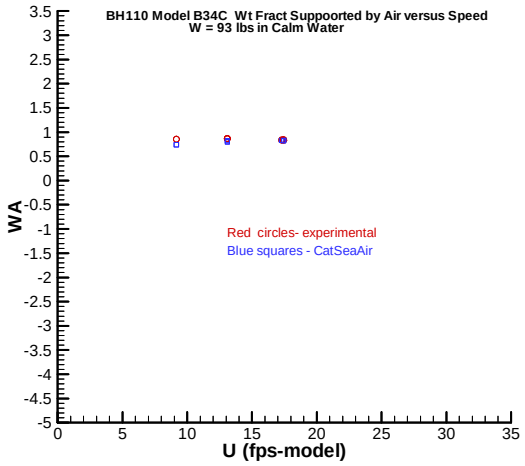

Fig 7: Calculated WA/W versus Model Speed for 93 lb Model

Another supportive CatSeaAir calculation is considered to be that of the calm-water drag. This is Figs 11, 12, and 13, in the same format as the preceding comparisons.

Drag, in representing craft resistance, is of primary importance in the calm-water performance prediction. It is also a second order variable and generally challenging to predict with accuracy.

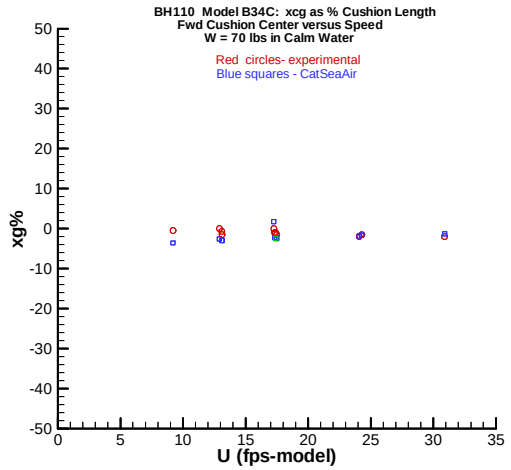

Fig 8: Calculated %xcg Versus Speed for 70lb Model

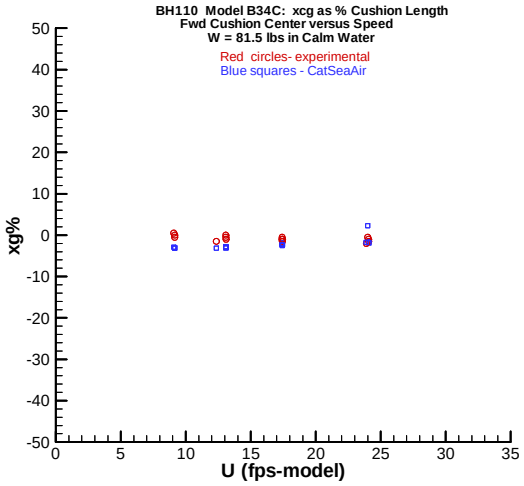

Fig 9: Calculated %xcg Versus Speed for 81.5lb Model

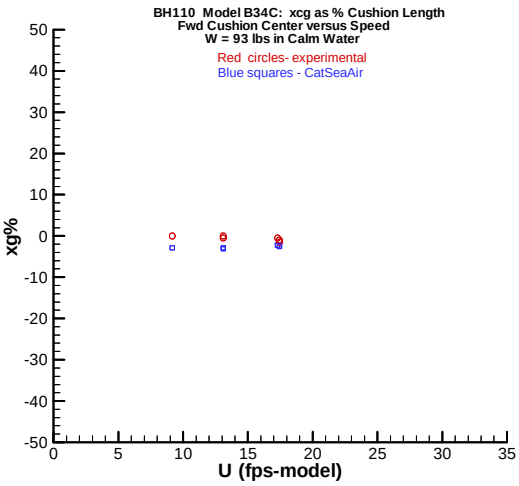

Figure 10: Calculated %xcg Versus Speed for 93lb Model

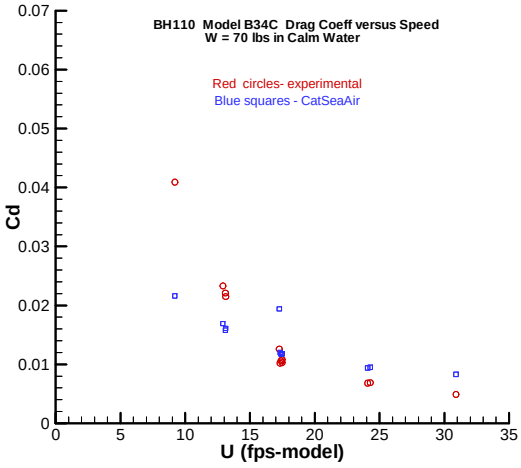

Figure 11: Calculated Cd Versus Speed for 70lb Model

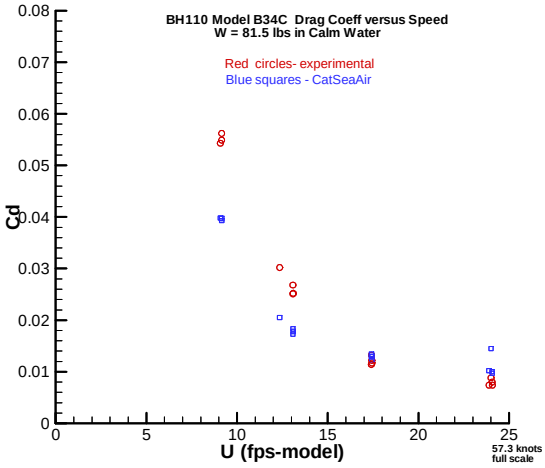

Figure 12: Calculated Cd Versus Speed for 81.5lb Model

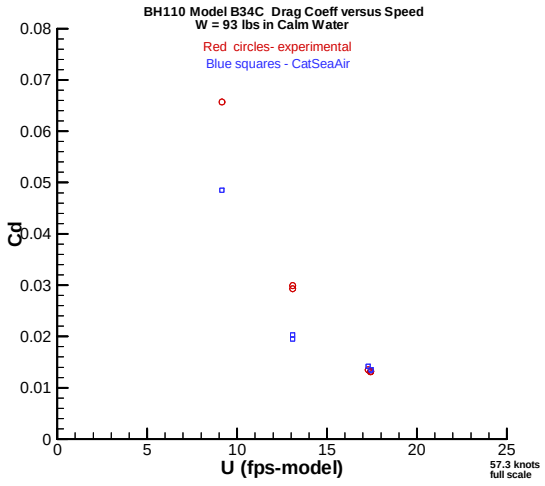

Figure 13: Calculated Cd versus Speed for 93lb Model

As a matter of record, the drag coefficient is by the previous definition:

$$C_d = \frac{drag}{\frac{1}{2}\rho U^2 Z_k} \qquad (10)$$

As these last three figures show, the calculated calm water drag is generally a little lower than the measured, but with the differences diminishing at the higher speeds. This is just as would be expected in consideration of the theory employed in CatSeaAir. The Maruo theory is a linearized theory and looses some effectiveness at lower Froude number corresponding to the lower speeds of the test series; 9 ft/sec was the lowest model speed tested. The length Froude number at U = 9 fps is .6, still high speed but associated with substantial wave-making and wave resistance. At the model speed of 30 fps, on the other-hand, Fn = 2, for which the wave making should be small and within the linearized theory. This is the observation in Figures 10 to 13.

Analysis versus Experiments - Seaway Dynamics

The principal test data reported from the seaway measurements were statistical accelerations at the bow, center of gravity, and transom.

The model test procedure was somewhat different than that of the calculation by CatSeaAir; the model was accelerated to speed in the fully-developed wave system and then measurements were made for a distance of 110 ft down the tank. The data was then statistically processed.

In the CatSeaAir calculations the model is started with the calm water equilibrium at the test speed and the wave system is ramped-up to the fully developed condition over a short time period. The statistical processing of the calculated data is delayed in the interest of achieving a statistically stationary response to the seaway.

The comparisons were limited to two of the seaway runs: #390 for Sea-State 2 and W = 70 lbs model weight and #438 for Sea-State 3 at W = 93 lbs model weight. The seaway runs were both fewer in number and time intensive to compute, as discussed. The speed for both runs is the design speed of nominally 17.45 fps (40 knots full scale). The starting calm-water runs are #393 at 70lbs and #437 at 93lbs. As shown on Table 1, the CG positions for these two cases are essentially identical; the calculated xcgc and WAc are used in all the seaway calculations. The results are summarized on Table 2 to follow.

There was a concern about achieving statistically stationary response from the numerical time-stepping solution in CatSeaAir, as well as in the model tests. The scaled Pierson-Moskowitz spectrum was inverted into the time domain for the time-stepping response solution by CatSeaAir. The wave input is thereby stationary random. The response output is meaningless as a statistical measure, e.g., RMS, unless it is likewise statistically stationary.

Figure 14 is a plot of calculated displacement response components of the Run #438 computation at SS3.

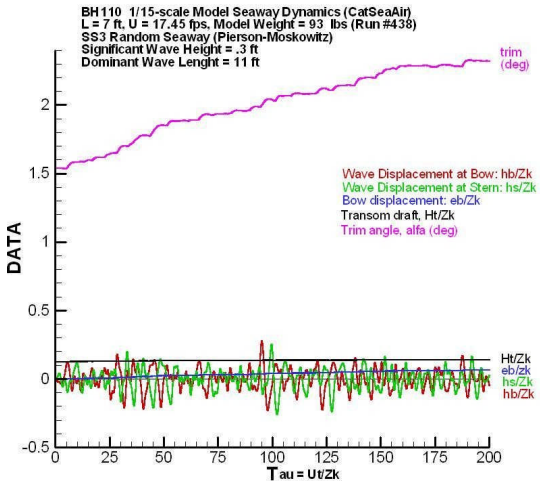

Fig 14: Displacement Distributions versus Time from Seaway Dynamic Analysis; Run 438, SS3, W = 93 lbs, U =17.43 fps, 10,000 time steps

The seawave dimensionless elevations at the bow and stern, as converted from the Pierson-Moskowitz spectrum with the .3 ft significant wave height (4.5 ft full scale), is plotted along the dimensionless time axis of Fig 14. The seaway is ramped-up as an inverse exponential from calm-water to its full stationary state at about $\tau = 10$, where the statistical data collection commences. Note that Ut is the distance the model has traveled down the tank. With the demi-hull keel offset Zk = 1.05 ft, $\tau = Ut/Zk = 10$ is slightly more than one model length of travel.

Figure 14 clearly shows that the model is predicted to have risen in the time mean, more in the bow than in the stern. This is because the wave pounding in slams is dominantly up, and dominantly in the bow, thus almost doubling the trim angle. The most relevant implication of Fig 14 is that the non-linear rise has essentially ceased at large time, which would imply that stationarity has been achieved. But it has taken 10,000 time steps at $\Delta\tau = .02$ to reach that state.

The companion SS2 time history (Table 2) although not shown, exhibits the same character, but converges to the apparent stationary random state slightly sooner.

Table 2: Seaway Dynamic Analysis – Calculations and Experiments

A. Run # 390 - SS2, U = 17.43 fps, W = 70 lbs

				RMS g's (CatSeaAir)			Mean (CatSeaAir)		
No.	**N**	**Tau**	**D (ft)**	**Bow**	**CG**	**Trans**	**Cl**	**Cd**	**L/D**
390	2500	50	52.5	0.485	0.103	0.254	0.229	0.0150	15.3
	5000	110	115.5	0.400	0.091	0.221	0.228	0.0135	16.8
	6000	120	126.0	0.420	0.095	0.246	0.228	0.0137	16.7
	8000	160	168.0	0.374	0.099	0.245	0.227	0.0130	17.4
	10000	200	210.0	0.351	0.101	0.240	0.227	0.0127	17.9
	From experiement						Calm Water Calculation		
390	4190	105	110.0	0.250	0.190	0.140	0.217	0.0117	18.4

B. Run # 438 - SS3, U = 17.43 fps, W = 93 lbs

				RMS g's (CatSeaAir)			Mean (CatSeaAir)		
No.	**N**	**Tau**	**D (ft)**	**Bow**	**CG**	**Trans**	**Cl**	**Cd**	**L/D**
438	3000	60	63.0	0.418	0.128	0.158	0.306	0.0297	10.3
	5000	110	115.5	0.390	0.129	0.160	0.305	0.0273	11.2
	6000	120	126.0	0.380	0.125	0.175	0.304	0.0258	11.8
	8000	160	168.0	0.381	0.123	0.175	0.304	0.0248	13.1
	10000	200	210.0	0.354	0.115	0.168	0.303	0.0231	21.2
	From experiement						Calm Water Calculation		
438	4190	105	110.0	0.520	0.330	0.210	0.286	0.0135	21.2

Turning to Table 2, the 10,000 time step analysis was done using the dump-restart capability of CatSeaAir for both of the calculations; the files are written on the dump and saved. The total of 10,000 time steps is accomplished in 5 segments for each of the runs A and B; the distance down the tank (D) corresponding to the advancing time is shown. It is being assumed that stationary response is achieved at 10,000 steps on the basis of Fig 14.

It is relevant to consider that the actual tank data collection was over 110 ft of tank length, with the measurements commencing from a transient start-up in the wave system.

But the 5^{th} – 7^{th} columns impact acceleration data of Table 2 would suggest that the stationary random state of the model response was hardly achieved in 110 ft.

The experimental statistics on RMS model acceleration is the last line in each of the Table 2 segments A and B. It is noteworthy that the Lockheed tank tests were done under Bell-Halter (now TEXTRON Marine and Land Systems) as an engineering design effort in the development of the BH110, and not as a research program. The model at 7 feet (1/15 scale) was really too small for the expectation of high absolute accuracy. Relative, rather than absolute, accuracy is needed for continuous improvement in design development. In view of both the experimental and numerical modeling uncertainties, the Table 2 comparisons are considered to exhibit supportive agreement.

One further Table 2 observation is worthy of attention. The right sides of the tables are calculated lift and drag coefficients. The upper-right sub-tables are the time means of the variations, with the last line being the calm-water calculated values of Table 1. There are no measurements available for the lift coefficients in the seaway. In this regard, the Cl might be expected to be close to the calm water value, even in waves. Cl is equivalent to the boat weight in calmwater. But continuing from Table 2B, for example, the predicted time mean Cl at $\tau = 200$ is 6% above the calm water Cl. It is this increased mean lift that produces the rise of the vessel above its calm water position, which is indicated and discussed on Figure 14.

The increase in mean drag over the calm water level indicated in Table 2 is believed to be consistent with expected levels of added resistance in waves. The drag increase is 71% over calm-water drag in the SS3 seaway at 40 knots full scale, by the predicted numbers of Table 2.

Hull Pressure and Structural Loading

It would seem inappropriate for a paper with “pressure and structural loading” featured in the title to not include material on pressure and structural loading. But pressure and structural loading was not part of the BH-110 experimental program, so there was nothing on this material to report from the focus of the work.

In the total development program, however, unsteady hull pressure distributions on a notional 10m bi-hull SES with B/L = .275 and Fn = 2.6 were evaluated. A sample of this is included here for the purpose of demonstrating the use of the extended CatSeaAir (EDITH 2-AG) code for dynamic load analysis in the seaway.

Fig 15 is the distribution of force coefficient, $C_f(x,\tau)$, corresponding to the predicted pressure sectionally integrated at the time $\tau = 50$ for the notional SES design at 75% cushion support.

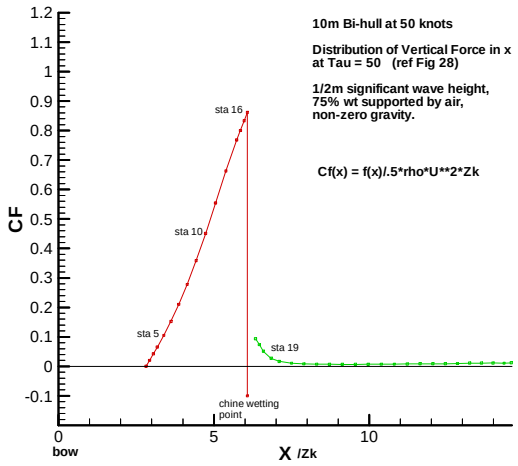

Fig 15: Vertical Force Distribution in x at time τ = 50 for 75% Cushion Support, Non-zero Gravity

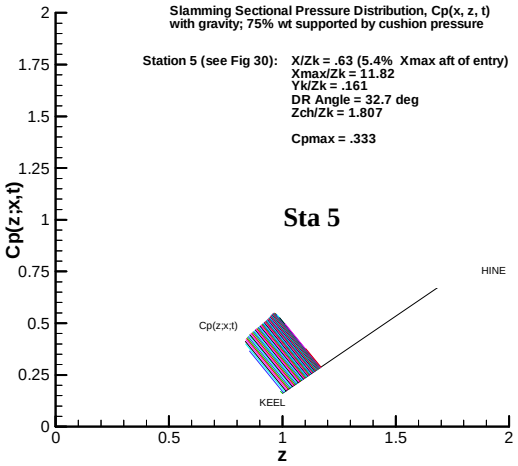

Fig 16: Half Demi-hull Section C_p(x, z, t) at Station 5, 5.4% of Wetted Length Aft of Entry (refer to Figure 15); 75% Wt by Cushion Pressure

The near discontinuity on Fig 15 is the occurrence of 'chine-wetting.' Just as in calm-water planning, the hull pressure (and lift) drop by an order of magnitude when the jet-head reaches the chine, proceeding outward. This is for the case of approximately cylindrical wetted geometry in x at chine-wetting and aft, which is the common case and the case here. Vessel-generated gravity waves then boost the pressure and lift aft in calm water. In the case of Fig 15 at τ = 50, the instantaneous motions and ambient waves, along with the cylindrical geometry, are responsible for almost nullifying the pressure loading aft.

The impact acceleration is largest at the bow around this time, implying high sectional and contour pressure loading there. Therefore, bow contour pressure distributions have been plotted at τ = 50 at each of the four sections marked on Fig 15. The pressure plots are Figs 16 through 19. The plots are transverse in z from the demi-hull keel to the chine with the heights of the bars representing the pressure magnitudes (The colors on Figures 16 through 19 are intended only to indicate the distribution of points at which the pressures were computed.) The vertical component of the integral of the pressure across the section at each of numbered stations is the values of the corresponding vertical-axis force coefficients on Fig 15.

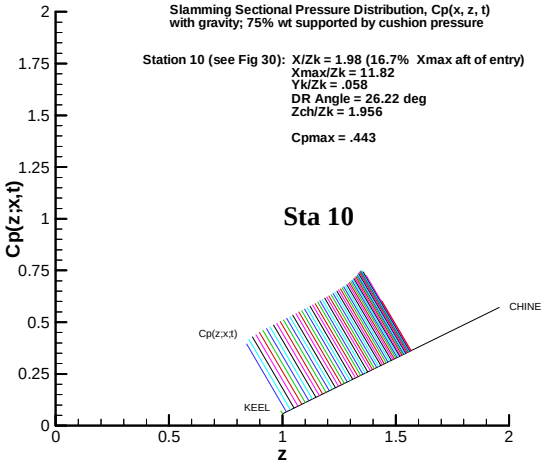

Figure 17: Half Demi-hull Section C_p(x, z, t) at Station 10, 16.7% of Wetted Length Aft of Entry (refer to Fig 15); 75% Wt by Cushion Pressure

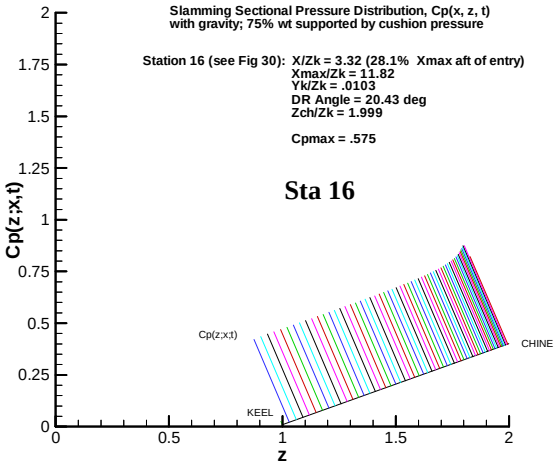

Figure 18: Half Demi-hull Section C_p(x, z, t) at Station 16, 28.1% of Wetted Length Aft of Entry (refer to Fig 15); 75% Wt by Cushion Pressure

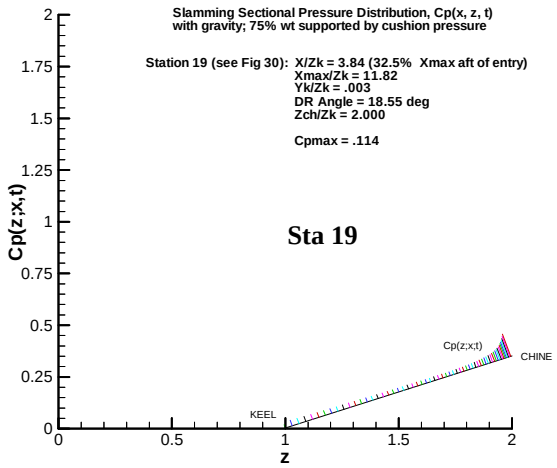

Figure 19: Half Demi-hull Section $C_p(x, z, t)$ at Station 19, 32.5% of Wetted Length Aft of Entry (refer to Fig 15); 75% Wt by Cushion Pressure

Recognize that Figs 16 through 19 are the pressures over the four section contours at a single time. The next time on the output record would show the pressures at the same sections slightly changed, and so forth. The time and spatially varying pressure field is available in this form for all times (10,000 steps) and for any of the 101 x-sections specified.

Conclusions

CatSeaAir is a computationally-intensive theoretical tool which has demonstrated useful agreement with the limited test data available. Pending further validation it could provide reliable prediction of structural loads on high-speed SES/Catamaran hull forms in a seaway.

It would be in order to further consider the quasi-steady approximation on wave effects employed for the time domain seaway dynamic analysis. It is not clear that this routine can be improved much for purposes of a design oriented computation tool for lifting hull forms. But its accuracy should be more thoroughly checked than time has yet permitted.

Probably of more importance is better treatment of the SES end seal leakage and drag. Seal drag has been included in CatSeaAir, but it is empirical, as deduced from past studies on operating SES craft. The air leakage rates largely determine the lift fan power. The drag equivalent to fan power was not included in the resistance estimates in the BH 110 model tests, and is therefore not an issue in the data comparisons of the last section. SES seal design reliability remains as a significant uncertainly in the technology of this very important craft type.

Acknowledgements

The authors have to thank primarily the Ship Structures Committee, who supported the work for two years; included, of course, is the US Coast Guard and the American Bureau of Shipping for their work in support of SSC.

The authors also thank Ms Leila Tahvildari at the University of New Orleans for her competence in producing the finished document.

This paper reflects the views of the authors and does not represent an official position, policy, or recommendation by the U.S. Coast Guard.

References

Von Karman, T. 1929 The impact of seaplane floats during landing. NACA TN 321 Washington, D.C., Oct.

Wagner, H. 1932 Uber stoss-und gleitvorgange an der oberflache von flussigkeiten. *Zeitschrift fur Angewandte Mathematik und Mechanik*, 12, 193, Aug.

Maruo, H. 1967 High and low-aspect ratio approximation of planing surfaces. *Schiffstechnik*, 72.

Tuck, E. 1975 Low-aspect ratio flat-ship theory. *Journal of Hydronautics*, 9, 1, January.

Stability and Seakeeping Tests with a 1/15 Scale Model of the Bell Aerospace Company Model B-34C, LMSC/D682700, December 1979.

Vorus, W. 1996 A flat cylinder theory for vessel impact and steady planing resistance. *Journal of Ship Research*, 40, 2, June.